

# The cytoplasmic filaments of the nuclear pore complex are dispensable for selective nuclear protein import

Tobias C. Walther,<sup>1</sup> Helen S. Pickersgill,<sup>2</sup> Volker C. Cordes,<sup>3,4</sup> Martin W. Goldberg,<sup>2</sup> Terry D. Allen,<sup>2</sup> Iain W. Mattaj,<sup>1</sup> and Maarten Fornerod<sup>1,5</sup>

<sup>1</sup>Gene Expression Program, EMBL, D-69117 Heidelberg, Germany

<sup>2</sup>Paterson Institute CRUK/CMB, M20 9BX Manchester, U.K.

<sup>3</sup>Karolinska Institute, S-17177 Stockholm, Sweden

<sup>4</sup>German Cancer Research Center, D-69120 Heidelberg, Germany

<sup>5</sup>Netherlands Cancer Institute H4, 1066 CX Amsterdam, Netherlands

The nuclear pore complex (NPC) mediates bidirectional macromolecular traffic between the nucleus and cytoplasm in eukaryotic cells. Eight filaments project from the NPC into the cytoplasm and are proposed to function in nuclear import. We investigated the localization and function of two nucleoporins on the cytoplasmic face of the NPC, CAN/Nup214 and RanBP2/Nup358. Consistent with previous data, RanBP2 was localized at the cytoplasmic filaments. In contrast, CAN was localized near the cytoplasmic coaxial ring. Unexpectedly, extensive blocking of RanBP2 with gold-conjugated antibodies failed to inhibit nuclear import. Therefore, RanBP2-deficient NPCs were generated by *in vitro* nuclear assembly in RanBP2-depleted *Xenopus* egg extracts. NPCs were formed that lacked cyto-

plasmic filaments, but that retained CAN. These nuclei efficiently imported nuclear localization sequence (NLS) or M9 substrates. NPCs lacking CAN retained RanBP2 and cytoplasmic filaments, and showed a minor NLS import defect. NPCs deficient in both CAN and RanBP2 displayed no cytoplasmic filaments and had a strikingly immature cytoplasmic appearance. However, they showed only a slight reduction in NLS-mediated import, no change in M9-mediated import, and were normal in growth and DNA replication. We conclude that RanBP2 is the major nucleoporin component of the cytoplasmic filaments of the NPC, and that these filaments do not have an essential role in importin  $\alpha/\beta$ - or transportin-dependent import.

## Introduction

The nuclear pore complex (NPC)\* is the mediator of all macromolecular transport between the nucleus and the cytoplasm of the eukaryotic cell. NPCs serve the cell's requirement for bidirectional, selective, diverse, and high-volume transport between these two compartments (for review see

Allen et al., 2000; Ryan and Wenthe, 2000; Fahrenkrog et al., 2001; Rout and Aitchison, 2001; Vasu and Forbes, 2001). Ultrastructural analyses of the NPC using transmission electron (Akey, 1989; Ris, 1989, 1991; Jarnik and Aebi, 1991; Hinshaw et al., 1992; Akey and Radermacher, 1993), scanning electron (Goldberg and Allen, 1993, 1996; Ris and Malecki, 1993; Ris, 1997), and atomic force (Rakowska et al., 1998; Stoffler et al., 1999b) microscopy has shown the vertebrate NPC to be an  $\sim 65$ -nm deep, plugged channel, decorated on each side with eight filaments attached to a coaxial ring that project away from the nuclear envelope (NE). Although the  $\sim 40$ – $50$ -nm filaments of the nuclear face join together at their distal ends to form a so-called nuclear basket or fishtrap (Goldberg and Allen, 1993, 1996; Ris and Malecki, 1993; Ris, 1997), the  $\sim 35$ – $50$ -nm filaments of the cytoplasmic side are not joined (Jarnik and Aebi, 1991; Goldberg and Allen, 1993).

Address correspondence to Maarten Fornerod, The Netherlands Cancer Institute H4, Plesmanlaan 121, 1066 CX Amsterdam, The Netherlands. Tel.: 31-20-512-2024. Fax: 31-20-512-2029. E-mail: fornerod@nki.nl

T.C. Walther and H.S. Pickersgill contributed equally to this work.

H.S. Pickersgill's present address is The Netherlands Cancer Institute H4, 1066 CX Amsterdam, The Netherlands.

\*Abbreviations used in this paper: AL, annulate lamellae; FEISEM, field emission in-lens scanning EM; mAb, monoclonal antibody; NE, nuclear envelope; NLS, nuclear localization sequence; NPC, nuclear pore complex; TEM, transmission EM.

Key words: nuclear pore complex; nuclear import; nuclear localization signal; RanBP2/Nup358; CAN/Nup214

In parallel to these structural studies, 30–40 different proteins, termed nucleoporins, have been identified as components of the NPC in vertebrates and yeast (Rout et al., 2000; Ryan and Wenthe, 2000; Fahrenkrog et al., 2001). To help understand the molecular organization of the NPC, these nucleoporins have been mapped to NPC subdomains using immunogold electron microscopy. In yeast, transmission EM (TEM) studies of protein A–tagged nucleoporins have shown that the majority of these map to both sides of the NPC (Rout et al., 2000). Exceptions that map exclusively to the cytoplasmic face are Nup159/Rat7 and Nup82 (Kraemer et al., 1995; Hurwitz et al., 1998; Rout et al., 2000). Even though regional information has been obtained for many nucleoporins, the rather low degree of structural definition of the NPC in transmission immuno-EM did not generally allow individual nucleoporins to be attributed to particular NPC substructures. In higher eukaryotes, three nucleoporins have been mapped to the cytoplasmic side of the NPC: CAN/Nup214 (Kraemer et al., 1994; Pante et al., 1994), Nup88/Nup84 (Bastos et al., 1997), and RanBP2/Nup358 (Wu et al., 1995; Yokoyama et al., 1995). RanBP2/Nup358, which has no identifiable yeast homologue, is the largest nucleoporin and has been localized to the cytoplasmic filaments of the NPC (Wilken et al., 1995; Wu et al., 1995; Yokoyama et al., 1995). It contains four RanGTP binding domains, highly similar in sequence to the one present in RanBP1. RanBP1 and isolated RanBP1-homologous domains of RanBP2 serve as Ran GTPase coactivators (Beddow et al., 1995; Bischoff et al., 1995; Richards et al., 1995; Schlenstedt et al., 1995; Villa Braslavsky et al., 2000), assisting the dissociation of RanGTP from importins (Bischoff and Gorlich, 1997; Floer et al., 1997; Schlenstedt et al., 1997) and exportin–cargo complexes (Kutay et al., 1998; Askjaer et al., 1999; Kehlenbach et al., 1999). RanBP2 also contains two Zinc fingers of the type predicted to bind RanGDP (Nakielny et al., 1999; Yaseen and Blobel, 1999b), and a number of loosely spaced FG repeats, providing potential binding sites for transport receptors. Furthermore, RanBP2/Nup358 serves as a binding site for the SUMO1-modified form of RanGAP1, the RanGTPase activating protein (Matunis et al., 1996, 1998; Mahajan et al., 1997). Recently, it has been shown that RanBP2 itself acts as an E3 ligase in the sumoylation reaction (Pichler et al., 2002). Purified RanBP2/Nup358 forms ~36-nm long, 5-nm thick filaments (Delphin et al., 1997), corresponding approximately to the size of the cytoplasmic filaments (Jarnik and Aebi, 1991), suggesting that RanBP2 could be the main constituent of the cytoplasmic NPC filaments.

CAN/Nup214 and Nup88/Nup84 form a cytoplasmically oriented nucleoporin subcomplex (Bastos et al., 1997; Fornerod et al., 1997). Based on immunogold EM studies (Kraemer et al., 1994; Pante et al., 1994), CAN/Nup214 is generally also referred to as a component of the cytoplasmic filaments. Genetic depletion of CAN/Nup214 in early mouse embryos resulted in reduced nuclear localization sequence (NLS)–mediated protein import, and strong nuclear poly(A)<sup>+</sup> RNA accumulation (van Deursen et al., 1996), whereas mutation of the *Drosophila* homologue of Nup88, *mbo*, results in a specific protein import defect without pronounced nuclear mRNA retention (Uv et al., 2000).

Several lines of evidence have suggested a role of the cytoplasmic filaments in nuclear import. EM analysis of nuclear import

of NLS-conjugated gold was found to involve multiple stages (Feldherr et al., 1984) that were subsequently specified as energy-independent binding (“docking”) of the import complex to the nuclear periphery and translocation to the nucleus (Newmeyer and Forbes, 1988; Richardson et al., 1988). Import complexes were enriched at fibrillar structures on the cytoplasmic face of the NPC (Newmeyer and Forbes, 1988; Richardson et al., 1988; Rutherford et al., 1997). Furthermore, it was found that inhibition of nuclear import by nonhydrolysable analogues of GTP lead to accumulation of RanGTP at the cytoplasmic filaments (Melchior et al., 1995). In vitro, RanGTP binds to RanBP2/Nup358 and stimulates binding of the NLS import receptor importin  $\beta$  to this nucleoporin (Melchior et al., 1995; Chi et al., 1996; Saitoh et al., 1996; Delphin et al., 1997; Yaseen and Blobel, 1999a). Antibodies to RanBP2-bound RanGAP1 reduced nuclear import efficiency, that could only be partially rescued by soluble RanGAP (Mahajan et al., 1997). These data were interpreted as evidence that RanBP2 serves as a docking site for incoming NLS import cargos, and that RanGTP played a controlling role in nuclear protein import (Melchior et al., 1995; Delphin et al., 1997; Mahajan et al., 1997; Yaseen and Blobel, 1999a). Observations of colloidal gold-labeled substrates during import showed association of the gold particles at two or three discrete sites of the cytoplasmic filaments (Akey and Goldfarb, 1989; Pante and Aebi, 1996), and filament bending toward the center of the NPC was reported (Pante and Aebi, 1996; Rutherford et al., 1997). It was suggested that docking of NLS cargos provokes the filaments to bend inwards and deliver them to the translocation channel. Cytoplasmic NPC filaments have also been proposed to contribute to excluding nonimport cargos from the nucleus by their Brownian movement (Rout et al., 2000). Antibodies to a large region of the RanBP2 protein inhibit import of an NLS-containing substrate (Yokoyama et al., 1995), strengthening the idea that RanBP2/Nup358 and the cytoplasmic NPC filaments play an essential role in nuclear import.

Biochemical depletion of nucleoporins from *Xenopus* egg extracts in which nuclear assembly on added chromatin templates takes place has been used to produce nuclei whose NPCs lack specific components (Finlay and Forbes, 1990; Finlay et al., 1991; Powers et al., 1995; Grandi et al., 1997; Walther et al., 2001). Here we address the question of the composition of the cytoplasmic filaments of the NPC and their role in nuclear import by analysis of two cytoplasmically oriented nucleoporins, CAN/Nup214 and RanBP2/Nup358. We find that whereas RanBP2/Nup358 is an essential part of the cytoplasmic filaments, CAN/Nup214 is not part of these structures. Surprisingly, given the indirect evidence for an import role cited above, NPCs lacking cytoplasmic filaments show no deficiency in NLS or M9 mediated nuclear accumulation, indicating that these structures have no essential function in the nuclear import of bulk import cargos.

## Results

### Immunoelectron microscopic localization of CAN/Nup214 and RanBP2/Nup358

The only three known vertebrate nucleoporins exclusively localized to the cytoplasmic face of the NPC are CAN/Nup214, Nup88, and RanBP2/Nup358, of which the former two form

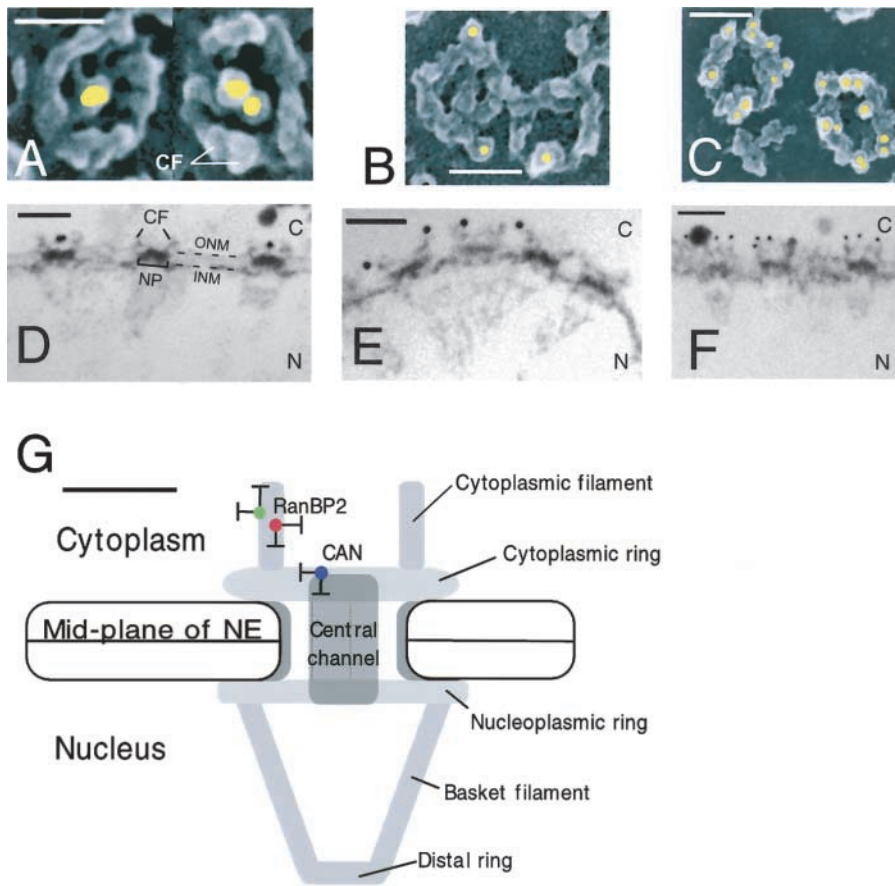


Figure 1. Isolated *Xenopus* oocyte NEs were fixed and labeled with affinity-purified anti-CAN or anti-RanBP2 antibodies, followed by 10-nm gold-conjugated secondary antibodies, and analyzed by FEISEM and TEM. (A–C) Representative FEISEM images of the cytoplasmic face of the NE labeled with 10-nm gold particles (artificially colored yellow) recognizing (A) anti-CAN/Nup214 antibodies; (B) anti-RanBP2/Nup358F antibodies; and (C) anti-RanBP2/Nup358V antibodies. Bars, 100 nm. (D–F) Representative TEM images of thin sections of the NE decorated with 10-nm gold labeling (D) anti-CAN/Nup214 antibodies; (E) anti-RanBP2/Nup358F antibodies; and (F) anti-RanBP2/Nup358V antibodies. CF, cytoplasmic filaments; NP, nuclear pore; ONM, outer nuclear membrane; INM, inner nuclear membrane; N, nucleus; C, cytoplasm. Bar, 100 nm. (G) Diagrammatical representation of the NPC summarizing the localization data for CAN/Nup214 and RanBP2/Nup358 using anti-RanBP2/Nup358F (green), anti-RanBP2/Nup358V (red), and anti-CAN/Nup214 (blue) antibodies. Putative positioning of substructures of the NPC are shaded in gray. Sizes and positions of substructures were derived from (Akey, 1989; Jarnik and Aebi, 1991; Akey and Radermacher, 1993; Goldberg and Allen, 1996) and our own measurements (unpublished data). Bar, 50 nm. Error bars represent standard deviations of the means.

a subcomplex. Because we intended to functionally characterize the role of the cytoplasmic filaments in nuclear transport, we first wished to reinvestigate the localization of RanBP2/Nup358 and CAN/Nup214 within the NPC. To this end we analyzed immunogold labeled *Xenopus laevis* oocyte NEs using field emission in-lens scanning EM (FEISEM), which provides a surface view of the NPC, and TEM, providing a cross-sectional view. For immunolocalization of RanBP2/Nup358, two polyclonal antibodies were used. One, anti-Nup358F, had been raised against a recombinant COOH-terminal segment, comprising amino acids 2501–2900 of the human homologue. The other, anti-Nup358V, was directed against amino acids 2285–2314 of human Nup358, of which residues 2290–2314 are identical in *Xenopus* and mammals. For immunolocalization of CAN/Nup214, polyclonal antibodies were raised against an NH<sub>2</sub>-terminal segment of the

*Xenopus* protein, comprising amino acids 1–213. All antibodies were affinity purified and recognized proteins of expected sizes in Western blots of *Xenopus* cell extracts (see Fig. 3 A).

For immuno-EM, isolated NEs were incubated with primary antibodies, followed by labeling with 10-nm gold-conjugated secondary antibodies. Representative images of FEISEM micrographs are shown in Fig. 1, A (CAN/Nup214), B (RanBP2/Nup358, antibody 358F), and C (RanBP2/Nup358, antibody 358V). The localization of at least 100 gold-labeled antibodies was determined for each nucleoporin by measuring the distance from the center of the NPC to the center of the gold-labeled antibodies. No significant labeling of the nuclear face was observed for any of the antibodies. The summary of the data collected for each of the three antibodies is shown in Table I. Anti-CAN/Nup214 antibody labeled

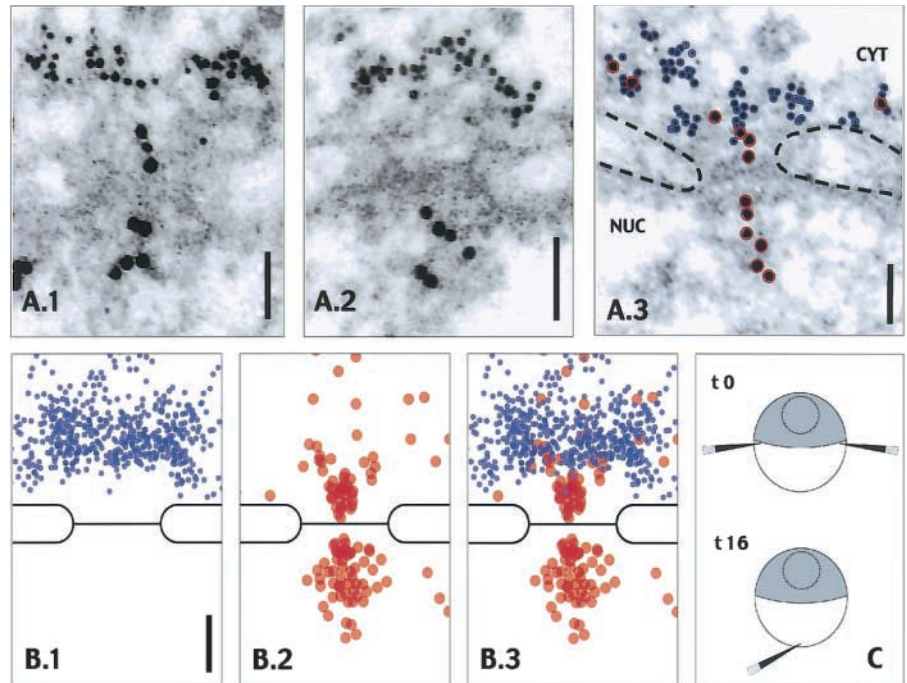
Table I. Summary of the localization of Nup214 and Nup358 using FEISEM and TEM

Antibody	SEM				TEM			
	Sample size (n)	Mean distance of gold from center of NPC (nm)	SD	SE	Sample size (n)	Mean distance of gold from midplane of NE (nm)	SD	SE
anti-214	106	11	9.3	0.90	36	31	5.7	0.95
anti-358F	229	39	10.3	0.68	50	57	10.9	1.54
anti-358V	114	31	12.0	1.12	56	51	10.0	1.34

The position of gold particles labelling CAN/Nup214 (anti-214) and RanBP2 (anti-358F and anti-358V) were determined in scanning EM and TEM.

**Figure 2. Antibodies specific for *Xenopus* RanBP2 label NPC-associated cytoplasmic filaments in vivo but do not prevent subsequent nuclear import of 10-nm gold particles coated with BSA-SV40NLS.**

(A) Transmission electron micrographs of ultrathin cross sections through NPCs of *Xenopus* oocytes after initial microinjection of 5-nm gold-coupled RanBP2/Nup358V antibodies and subsequent injection of 10-nm gold-coupled BSA-NLS. In all images, cytoplasm (CYT) and nuclear interior (NUC) adjacent to the nuclear envelope are oriented to the top and bottom, respectively. In A.3, the 5-nm gold grains which are coupled to the RanBP2 antibodies decorating the NPC-attached cytoplasmic fibrils are highlighted with blue circles; red circles mark the 10-nm gold grains coated with BSA-NLS. (B) Relative distribution of 5- (blue) and 10-nm gold particles (red) with respect to an idealistic NPC in cross section. Signals were assembled from 15 representative NPC images. Note that the distance between the peak distribution of the 5-nm gold particles and the central midplane of the NPC is  $\sim 70$  nm, whereas an area more proximal to the midplane (distance from 45 to 0 nm) is essentially devoid of 5-nm gold grains. Note further that 10-nm gold particles most proximal to the midplane are found only near the central "channel" region of NPC. Bars, 50 nm. (C) Schematic representation of sequential injections of antibodies and transport substrate into stage VI oocytes. Primary injections ( $t_0$ ) with 5-nm gold anti-RanBP2, or with buffer alone for mock injections, were at two opposite sites of the equatorial borderline between the oocyte's hemispheres. Subsequent injections of 10-nm-gold BSA-SV40NLS ( $t_{16}$ ) were into the vegetal hemisphere. Oocytes were further incubated and processed for electron microscopy.



centrally, at a mean distance of 11 nm ( $\pm$  SE 0.9) from the center of the NPC, corresponding to the inner aspect of the cytoplasmic ring or the cytoplasmic entrance of the translocation channel. In contrast, both anti-Nup358 antibodies labeled more peripheral structures of the NPC, at a mean distance of 39 nm  $\pm$  0.68 for anti-Nup358F, and 31 nm  $\pm$  1.12 for anti-Nup358V, corresponding to a position on the cytoplasmic filaments.

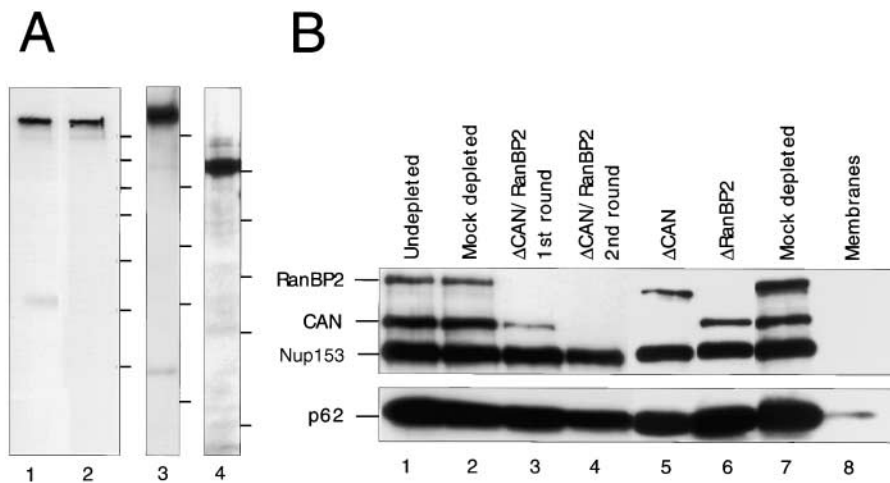
To obtain measurements along the central axis, isolated NEs were labeled with anti-CAN/Nup214, anti-RanBP2/Nup358F (Fig. 1 E), and anti-RanBP2/Nup358V (Fig. 1 F), and processed for visualization using TEM. Gold particle distribution in cross-sectional images through the NE was measured as distance from the NE midplane. Again, Nup214 labeling was found closer to the core structures of the NPC, with a mean distance of 31 nm  $\pm$  0.95 ( $n = 36$ ). In contrast, Nup358F labeling was at a mean distance of 57 nm  $\pm$  1.54 ( $n = 50$ ), and Nup358V labeling was found significantly more proximal to the NE at a mean distance of 51  $\pm$  1.34 nm ( $n = 56$ ;  $P < 0.01$ ).

As summarized in Table I and Fig. 1 G, a significant difference between the distribution of labeling of CAN and RanBP2 was observed, with the anti RanBP2 antibodies labeling more peripherally and deeper into the cytoplasm. Compared with the labeling for CAN/Nup214, the anti-Nup358 labeling generally resulted in a wider data spread. These data indicate that RanBP2 but not CAN localizes to the cytoplasmic filaments of the NPC, and suggest that the COOH terminus of RanBP2 is oriented toward the cytoplasm.

### In vivo decoration of cytoplasmic NPC filaments with RanBP2 antibodies does not prevent NLS-mediated nuclear import in *Xenopus* oocytes

As a first approach to assess a possible involvement of the cytoplasmic filaments in nuclear protein import, we attempted to sterically occlude these filaments in vivo, and thus prevent them from binding partner proteins. To this end, high concentrations of anti-Nup358V were injected into the cytoplasm of living *Xenopus* oocytes. These injections resulted in antibody sequestration at the cytoplasmic fibers bound either to NPCs or the pore complexes of the annulate lamellae (AL) (see below; Cordes et al., 1997a). At later time points, the same cells were reinjected with transport substrates, incubated further, and finally analyzed for nuclear import. Given that a stage VI oocyte contains an average total of  $\sim 2.4 \times 10^8$  pore complexes ( $\sim 80\%$  of which are AL pore complexes, 20% NPCs; Cordes et al., 1995), and supposing that maximally 16 copies of RanBP2 are present per pore complex, the upper value of RanBP2 copies per oocyte, including a minor pool of soluble RanBP2, can be estimated at  $\sim 4 \times 10^9$ . To be able to saturate this cellular pool of RanBP2, affinity-purified antibodies in initial experiments were injected at concentrations which resulted in a  $>10^2$ -fold molar surplus of antibody to RanBP2 in the oocyte. No inhibitory effects on BSA-NLS import were observed (unpublished data; Cordes et al., 1997a).

These investigations did not rule out that some NPCs had escaped immunoblocking and were still capable of RanBP2-mediated nuclear protein import. To visualize the effect of RanBP2 antibody-binding on nuclear translocation through individual NPCs, subsequent microinjection



prolonged exposure (unpublished data). Positions of marker proteins of 250, 150, 100, 75, 50, 37, and 25 kD are given at the right margins. (B) Monoclonal 414 immunoblot of undepleted (lane 1), or immunodepleted (lanes 2–7) fractionated *Xenopus* egg extracts as indicated above the lanes. (Lane 8) Fractionated membranes. Positions of RanBP2/Nup358, CAN/Nup214, Nup153, and p62 are indicated on the left.

experiments were performed with RanBP2 antibodies coupled to 5-nm gold, and the transport cargo BSA-NLS was coated onto 10-nm gold particles. As illustrated in Fig. 2 C, the gold-coupled RanBP2 antibodies were injected into the cytoplasm of several oocytes first, followed by several hours incubation to allow sequestration of antibodies at the nuclear periphery as confirmed by electron microscopy of some oocytes fixed directly afterwards (see Materials and

methods; Cordes et al., 1997a). The remaining oocytes were reinjected with the 10-nm gold-coupled transport cargo and later fixed and processed for TEM.

A selection of resulting micrographs is shown in Fig. 2 A. The 5-nm gold-coupled RanBP2 antibodies specifically accumulated at the cytoplasmic side of the NE, often densely decorating the cytoplasmic fibrils projecting from the NPCs. After prolonged incubation, RanBP2 antibod-

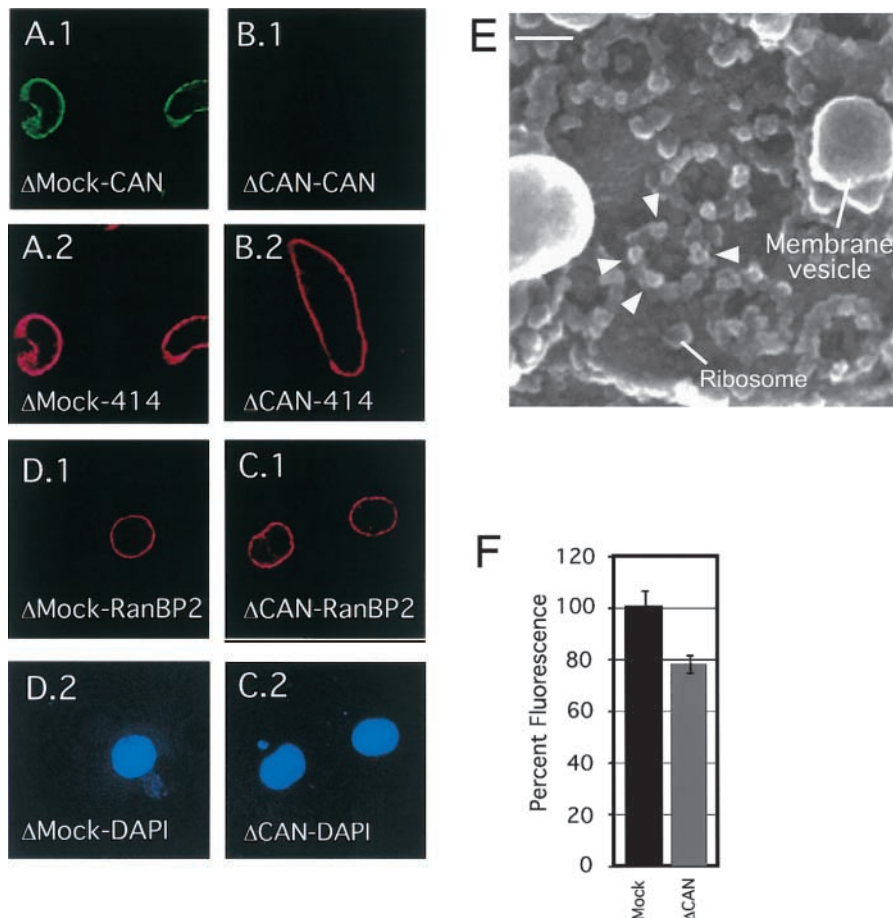
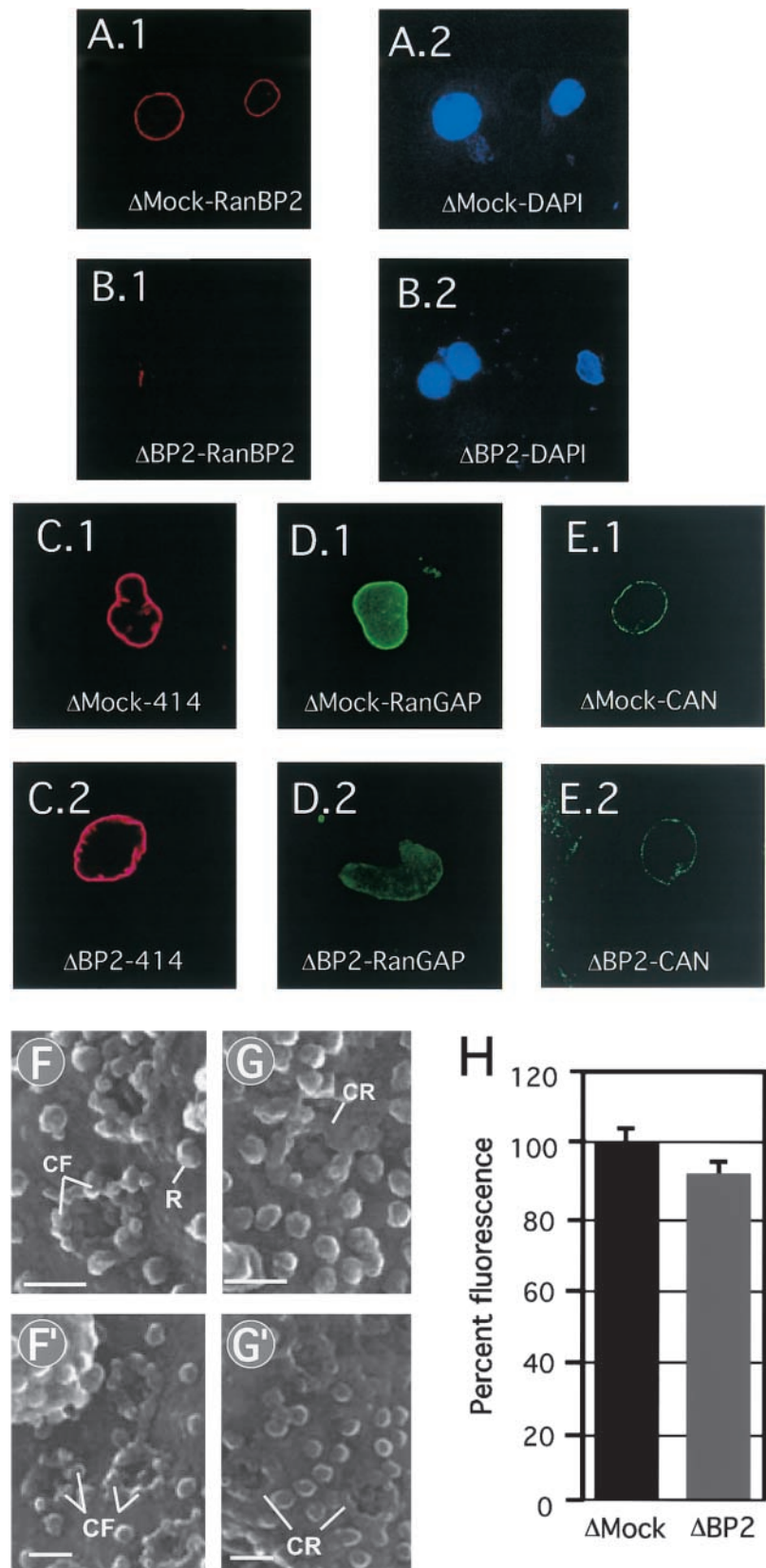


**Figure 4. CAN/Nup214-deficient NPCs.** (A–D). Nuclei that lack CAN/Nup214 retain RanBP2/Nup358. In vitro formed nuclei from mock-depleted (A and D) or CAN/Nup214 depleted (B and C) *Xenopus* egg extracts were stained with anti-CAN/Nup214 (A.1 and A.2), anti-RanBP2/Nup358 (C.1 and C.2), monoclonal 414 (A.2 and B.2), and DAPI (C.2 and D.2). (E) CAN/Nup214-deficient NPCs retain cytoplasmic filaments. Nuclei formed from CAN/Nup214-depleted egg extracts were imaged from the cytoplasmic side using FESEM. Arrowheads indicate cytoplasmic filaments. Bar, 100 nm. (F) CAN/Nup214-deficient nuclei show nuclear import of BSA-NLS to be reduced to 75% of control levels. In vitro assembled nuclei from mock or CAN/Nup214 ( $\Delta$ CAN)-depleted egg extracts were incubated with FITC- and TRITC-labeled BSA-SLN. After 30 min of import, nuclei were fixed and the intranuclear FITC signal quantified. A minority of nuclei that showed TRITC signal were excluded from the analysis. Bars represent standard errors of means.

**Figure 5. RanBP2/Nup358-deficient NPCs.** (A–E) Nuclei that lack RanBP2/Nup358 retain CAN/Nup214 but lack RanGAP1. In vitro formed nuclei from mock-depleted (A.1, A.2, C.1, D.1, and E.1) or RanBP2/Nup358-depleted (B.1, B.2, C.2, D.2, and E.2) *Xenopus* egg extracts were stained with anti-Nup358V (A.1 and B.1), monoclonal 414 (C.1 and C.2), anti-RanGAP1 (D.1 and D.2), and anti-CAN/Nup214 (E.1 and E.2), and DAPI (A.2 and B.2). Representative images are shown. (F–G) RanBP2/Nup358 deficient NPCs lack cytoplasmic filaments. Nuclei formed from mock-depleted (F and F') or RanBP2/Nup358-depleted (G and G') egg extracts were imaged from the cytoplasmic side using FEISEM. CF, cytoplasmic filament; CR, cytoplasmic ring; R, ribosome. Bars, 100 nm. (H) RanBP2/Nup358-deficient nuclei show normal nuclear import of BSA-NLS. In vitro assembled nuclei from mock- ( $\Delta$ Mock) or RanBP2/Nup358- ( $\Delta$ BP2) depleted egg extracts were assayed for nuclear import as described in Fig. 4.



ies were not only found attached to these NPC-proximal fibrils alone, but started to sequester within a region of up to 500 nm surrounding the nucleus (unpublished data). With the exception of the dense labeling of the AL pore complexes described earlier (Cordes et al., 1997a), no ac-

cumulation of 5-nm gold grains were seen in cytoplasmic areas more distal from the NE. 5-nm gold grains were not detectable in the nuclear interior. 10-nm gold-labeled BSA-NLS particles were enriched at NPCs (Fig. 2 A) and AL pore complexes (unpublished data; Cordes et al.,

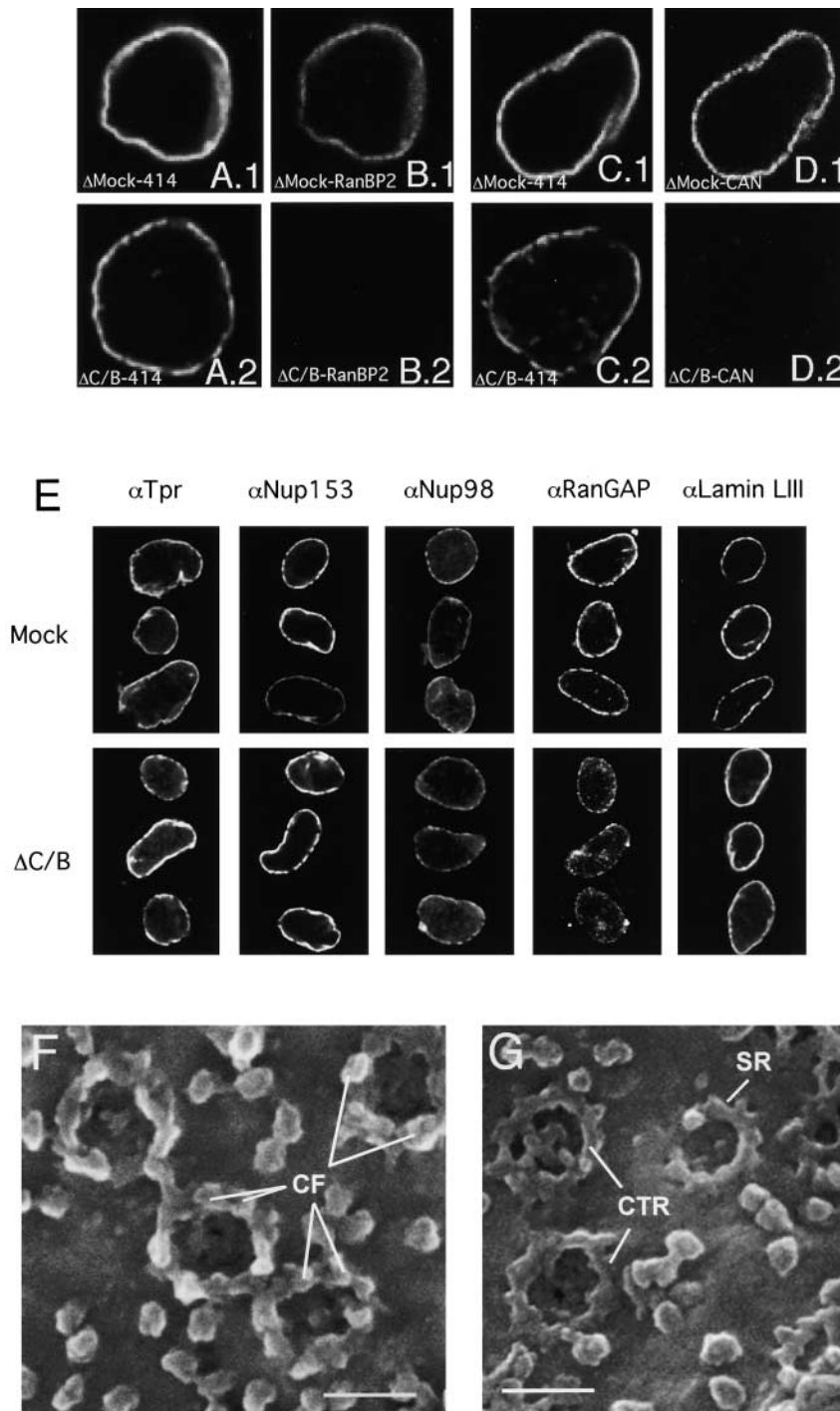


**Figure 6. CAN/Nup214- and RanBP2/Nup358-deficient NPCs.** (A–D) Formation of nuclei that lack both CAN/Nup214 and RanBP2/Nup358. In vitro formed nuclei from mock-depleted (A.1, B.1, C.1, D.1) or CAN/RanBP2-depleted (A.2, B.2, C.2, D.2) *Xenopus* egg extracts were stained with monoclonal 414 (A and C), anti-Nup358V (B), and anti-CAN/Nup214 (D). Representative images are shown. (E) CAN and RanBP2-deficient nuclei retain nuclear NPC components and a nuclear lamina. Assembled nuclei as above were immunostained with antibodies to Tpr, Nup153, Nup98, RanGAP1, and Lamin LIII. (F and G) RanBP2/Nup358-deficient NPCs lack cytoplasmic filaments and show an immature cytoplasmic ring. Nuclei formed from mock- (F) or CAN/RanBP2-depleted (G) egg extracts were imaged from the cytoplasmic side using FEISEM. CF, cytoplasmic filaments; CTR, cytoplasmic thin rings; SR, star ring. Bar, 100 nm.

1997a), and were also found throughout the nuclear interior, independently of whether cells had initially been injected with RanBP2 antibodies or mock injected with buffer alone. Despite this dense decoration of the cytoplasmic fibrils with 5-nm gold grains, the 10-nm gold particles in such NPCs were found at both the outer and inner side of the cross-sectioned electron-dense central midplane (Fig. 2 B). This indicated that the central translocation site within the NPC had remained accessible for even large cargo molecules (the diameter of a BSA-coated 10-nm gold grain can reach  $\sim 16$  nm) and capable of mediating nuclear import.

#### Immunodepletion of CAN/Nup214 and RanBP2/Nup358 from *Xenopus laevis* egg extracts

To more directly assess the role of CAN and RanBP2 in nuclear import, we made use of in vitro nuclear assembly using CAN and/or RanBP2 immunodepleted *Xenopus laevis* egg extracts (Finlay and Forbes, 1990). Affinity-purified anti-CAN, anti-RanBP2 (358V), or a mixture of the two antibodies were crosslinked to protein A Sepharose, and 400  $\mu$ l of fractionated interphase egg cytosol was subjected to two rounds of immunodepletion (Fig. 3). Western blot analysis of single- or double-depleted extracts probed with monoclonal antibody (mAb) 414 showed a very efficient and specific removal of

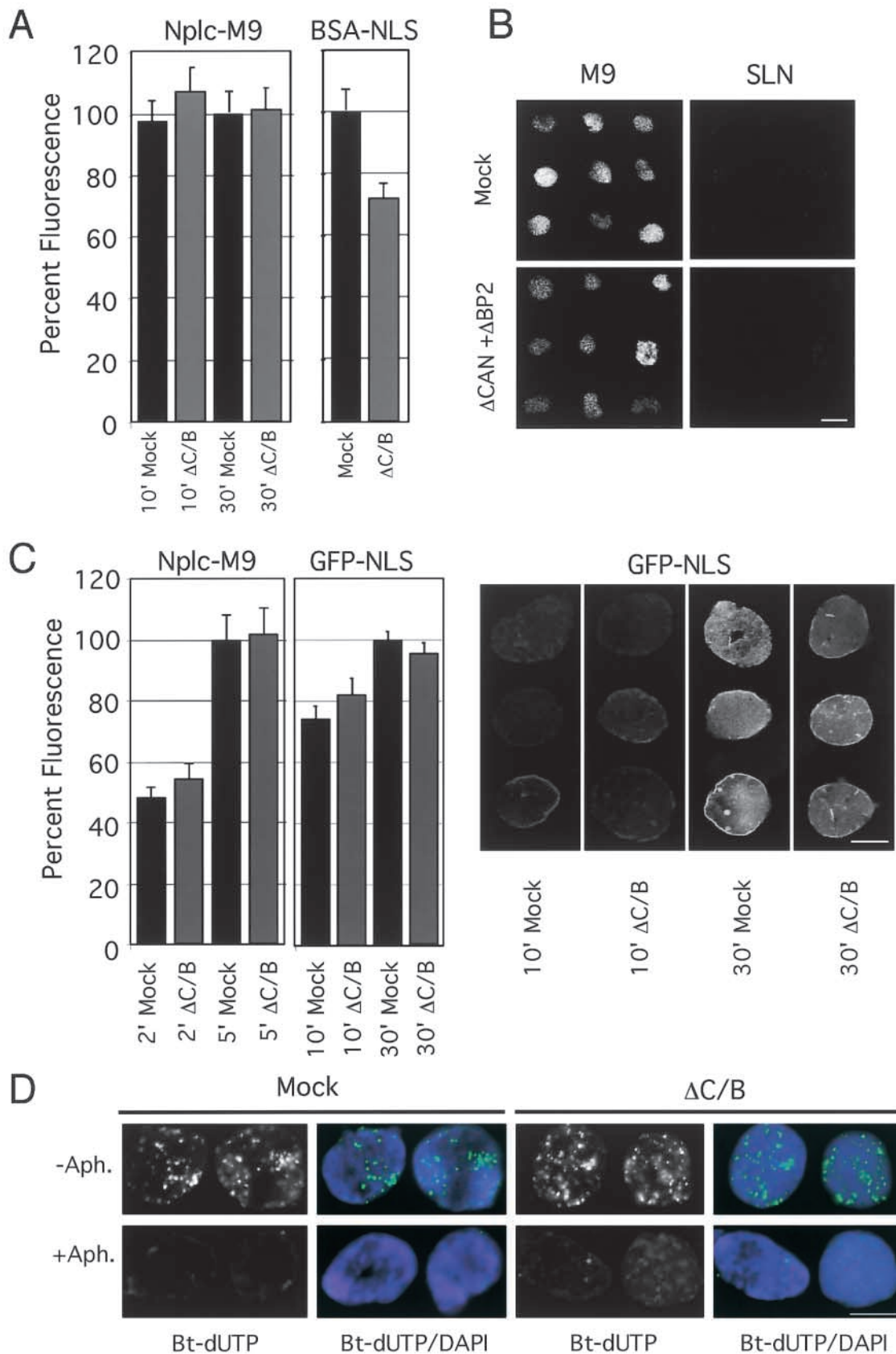


**Figure 7. Nuclear import in CAN- and RanBP2-deficient nuclei.** (A) CAN/RanBP2-deficient nuclei show normal nuclear import of Nplc-M9 and slightly reduced import of BSA-NLS. In vitro assembled nuclei from mock- (Mock) or CAN/RanBP2- ( $\Delta C/B$ ) depleted egg extracts were incubated with FITC-labeled Nplc-M9 or BSA-NLS. After 10 and 30 min (M9) or 40 min (NLS) of import, nuclei were fixed and intranuclear FITC signal was quantified as in Fig. 4. (B) CAN/RanBP2-deficient nuclei are not hyperpermeable. Random samples of nuclei from A. (M9) were analyzed for exclusion of BSA-SLN. No difference regarding nuclear exclusion of BSA-SLN was observed between mock-depleted and

CAN (Fig. 3, lane 5), RanBP2 (Fig. 3, lane 6), and both CAN and RanBP2 (Fig. 3, lane 4). Complete removal of nucleoporins using this method usually requires two rounds of depletion (Fig. 3, compare lanes 3 and 4; unpublished data). No CAN or RanBP2 was detected in the *Xenopus* egg membrane fraction (Fig. 3, lane 8) or demembrated sperm chromatin (Walther et al., 2001). Nontargeted nucleoporins were still present in depleted extracts (Fig. 3, lanes 4–6); however, a small fraction of p62 was consistently codepleted with CAN (Fig. 3, lanes 4 and 5; unpublished data). Mock-depleted extracts were not affected in mAb414-reactive nucleoporin composition (Fig. 3, compare lanes 1 and 2).

### CAN/Nup214-deficient nuclei retain cytoplasmic filaments and have a slight nuclear import defect

CAN/Nup214-depleted extracts supported efficient nuclear formation when combined with a membrane fraction, demembrated sperm chromatin, and an ATP regenerating system (Fig. 4, B.2 and C.2). As expected, no CAN/Nup214 was detected at the nuclear rim of CAN-deficient nuclei (Fig. 4, compare B.1 with A.1), whereas mAb414 staining appeared unaffected (Fig. 4, compare B.2 with A.2). Despite the absence of CAN, RanBP2 localized normally at the NE (Fig. 4, compare C.1 with D.1), consistent with localization of both proteins at separate substructures of the NPC. High-resolution FEISEM images of the cytoplasmic surface of CAN/Nup214 deficient NPCs showed that cytoplasmic filaments were present (Fig. 4 E, arrows), further supporting the notion that CAN/Nup214 is not part of these substructures or required for their formation. Internal structures were apparent but difficult to resolve, and it was not possible to determine whether there were any internal structural abnormalities.

Previously, genetic depletion of CAN/Nup214 in early mouse embryos had been shown to result in an ~50% reduced efficiency of nuclear import of a reporter NLS protein (van Deursen et al., 1996). Here we tested whether nuclear import of an FITC-labeled nuclear import substrate, consisting of 10 copies of the SV40 large T NLS crosslinked to BSA was affected. As shown in Fig. 4 F, we detected a reduction of the level of import of this substrate to ~75% of control levels.

### RanBP2/Nup358-deficient nuclei lack cytoplasmic filaments and import efficiently

Similar to CAN/Nup214-deficient nuclei, RanBP2/Nup358-deficient nuclei formed efficiently from depleted extracts (Fig. 5, B.2–E.2). No RanBP2 could be detected at the NE of these nuclei (Fig. 5 B.1), in contrast to the presence of RanBP2 in nuclei formed from mock-depleted extracts (Fig. 5 A.1). In *Xenopus* egg extracts, RanGAP1 is mainly present in its sumoylated form, a modification that targets the protein to RanBP2 (Mahajan et al., 1997; Matunis et al., 1998), resulting in a nuclear rim localization (Fig. 5 D.1). Consistently, strong RanGAP1 labeling at the nuclear rim was

found in control nuclei, but was reduced in RanBP2-deficient NPCs (Fig. 5 D.2). In contrast, no reduction in staining intensity with mAb414 (Fig. 5 C.2) or anti-CAN (Fig. 5 E.2) was apparent. Also, the level of anti-CAN immunogold labeling in FEISEM analysis of these nuclei was not reduced (unpublished data).

High-resolution FEISEM of the cytoplasmic face of the RanBP2-deficient nuclei showed that the NPCs (Fig. 5 G and G') were structurally different than the mock-depleted controls (Fig. 5, F and F'), and that only the coaxial cytoplasmic ring, but not the filaments, was still visible. However, in the absence of cytoplasmic filaments, nuclear import of BSA-NLS (Fig. 5 H) or nucleoplasmin core M9 (unpublished data; see below) was not significantly affected (Fig. 5 H). Nuclear import was signal dependent, as BSA coupled to a nonfunctional "reverse NLS" peptide was excluded from RanBP2 deficient nuclei (see below).

### CAN/Nup214- and RanBP2/Nup358-deficient nuclei exhibit aberrant NPC morphology but show no further import defect

Combined CAN/Nup214- and RanBP2/Nup358-depleted nuclei also efficiently formed in the nuclear assembly reaction (Fig. 6, A–D). As expected, both CAN and RanBP2 were absent from the double-deficient NEs (Fig. 6, B and D), whereas mAb414 staining appeared only partially reduced (Fig. 6, compare A.1 and A.2 or C.1 and C.2). No reduction was detected in the staining for nucleoporins Tpr, Nup153, and Nup98 (Fig. 6 E). These nucleoporins are localized at the nuclear face of the NPC (Sukegawa and Blobel, 1993; Radu et al., 1995; Cordes et al., 1997b; Walther et al., 2001), and their presence indicates that the structure of the nuclear side of NPCs was not affected. RanGAP1 staining (Fig. 6 E) was reduced to a similar level as in the RanBP2 single-deficient nuclei (Fig. 5 D.2). No difference was detected in the levels of Lamin LIII (Fig. 6 E), indicating that the CAN- and RanBP2-deficient nuclei were able to assemble a nuclear lamina. Nuclear growth that is suggested to be dependent on a functional nuclear lamina (Meier et al., 1991; Spann et al., 1997; Yang et al., 1997), also appeared normal as the average size of mutant nuclei (diameter  $14.8 \pm 0.5 \mu\text{m}$ ) was similar to control nuclei ( $15.6 \pm 0.6 \mu\text{m}$ ). FEISEM imaging of the cytoplasmic surface of the double-deficient nuclei revealed a striking structural NPC phenotype (Fig. 6 F and G). None of the NPCs visualized appeared completely assembled; instead, most had either only a star ring or a cytoplasmic thin ring, which have been recognized as NPC assembly intermediates (Goldberg et al., 1997). The tips of some of the star ring subunits appeared to be buried in the NE as previously described (Fig. 6 G, arrow). No obvious cytoplasmic coaxial rings or cytoplasmic filaments were present.

CAN/RanBP2-deficient nuclei. (C) Initial rates of transportin- and importin  $\alpha/\beta$ -mediated import are unaffected by absence of CAN and RanBP2. Mock- or CAN/RanBP2-deficient nuclei were incubated with FITC-labeled nucleoplasmic core M9 (Nplc-M9) or GFP-NLS. After 2 and 5 min (M9) or 10 and 30 min (NLS) of import, nuclei were fixed and intranuclear FITC signal was quantified as in Fig. 4. Representative images are shown to the left. (D) CAN and RanBP2-deficient nuclei are DNA replication competent. Mock- or CAN/RanBP2-deficient nuclei were assembled in the presence of 40  $\mu\text{M}$  21-biotin dUTP (Bt-dUTP) and in the presence or absence of 14  $\mu\text{M}$  aphidicolin (Aph.) as indicated. Nuclei were fixed and stained with Alexa 488-labeled streptavidin (green) and DAPI (blue). Bars, 10  $\mu\text{m}$ .

In spite of the strikingly aberrant cytoplasmic phenotype of the CAN/Nup214 and RanBP2/Nup358 double-deficient NPCs, import of BSA-NLS was only reduced to ~70% of control levels (Fig. 7 A) similar to the reduction observed for the CAN/Nup214 single-depleted nuclei (Fig. 4 G). Import of fluorescently labeled Nplc-M9 (Englmeier et al., 1999) was equally efficient in nuclei formed from CAN/RanBP2 double- or mock-depleted extract (Fig. 7 A). Nuclear import into CAN- and RanBP2-deficient nuclei was signal dependent, as the inert control substrate BSA-“reverseNLS” (BSA-SLN) was equally well excluded from controls as from the double deficient nuclei (Fig. 7 B). To test for possible kinetic differences in nuclear protein import between control and CAN/RanBP2-deficient nuclei, nuclear accumulation of Nplc-M9 and GFP-NLS was measured at early time points (2 and 10 min, respectively) after substrate addition. As shown in Fig. 7 C, no differences in import rates were measured between nuclei formed from mock- and CAN/RanBP2-depleted extracts. Note that compared with the multivalent BSA-NLS substrate (Fig. 7 A), nuclear import of the smaller, monovalent GFP-NLS import substrate in CAN- and RanBP2-deficient nuclei was less affected.

Synthetic nuclei are able to initiate a single round of semi-conservative DNA replication (Blow and Laskey, 1986), which is dependent on their ability to concentrate factors for DNA replication (Walter et al., 1998). As a functional test for import of natural cargos, we assayed incorporation of the thymidine analogue 21-biotin-dUTP into the DNA of nuclei lacking CAN and RanBP2. As shown in Fig. 7 D, both mutant and control nuclei showed a similar level of diffuse nuclear staining with numerous bright foci. The majority of this signal was absent when DNA polymerase  $\alpha$  was inhibited by aphidicolin (Fig. 7 D), indicating that the signal resulted from DNA replication. We conclude that in the absence of CAN and RanBP2, nuclei are capable of normal accumulation of replication factors.

## Discussion

In this study, we assessed the function of the cytoplasmic NPC filaments in nuclear protein import. Previously, the cytoplasmic filaments have been implicated in protein import due to their colocalization with injected NLS-gold conjugates, association with RanGTP and importin  $\beta$ , by antibody inhibition experiments, and because of their potential to exclude macromolecules with no affinity for nucleoporins (Melchior et al., 1995; Yokoyama et al., 1995; Pante and Aebi, 1996; Mahajan et al., 1997; Rutherford et al., 1997; Yaseen and Blobel, 1999a; Rout et al., 2000).

### The composition of the cytoplasmic filaments

Two proteins are commonly referred to as components of the cytoplasmic filaments, RanBP2/Nup358 and CAN/Nup214 (Ohno et al., 1998; Stoffler et al., 1999a; Allen et al., 2000). Our localization of CAN places it away from the filaments, near the cytoplasmic entrance of the translocation channel. This conclusion is derived from three observations. First, we have used a high resolution scanning immuno-EM technique that allows simultaneous visualization of the cytoplasmic surface of the NPC and CAN/Nup214-reactive im-

munogold labeling and thereby shown a localization of CAN close to the center of the NPC. Second, transmission immuno-EM analysis shows labeling of CAN/Nup214 at a position close to the center of the NPC rather than a localization at the cytoplasmic filaments. Third, immunodepletion of RanBP2/Nup358 resulted in formation of NPCs lacking cytoplasmic filaments, yet CAN/Nup214 remained present on these NPCs. The immature phenotype of the cytoplasmic rings in NPCs codepleted for CAN and RanBP2, as compared with RanBP2-deficient ones, further argues for a localization of CAN/Nup214 near the cytoplasmic ring rather than on the filaments.

In two previous studies using TEM, it had been concluded that Nup214 is a component of the cytoplasmic filaments (Kraemer et al., 1994; Pante et al., 1994). However, the images presented in one of these studies (Kraemer et al., 1994) revealed a localization that is consistent with ours, using an antibody directed to a central domain of CAN. From the position of the 11 gold particles presented in their study, a mean distance of 27 nm ( $\pm$  a standard deviation of 7) from the midplane of the NE and 10 nm  $\pm$  7 from the center of the NPC can be determined. These values lie within the spread, and even within the error of our localization data. The second study, using a serum against full-length native rat protein, presented conclusive labeling of the cytoplasmic filaments (Pante et al., 1994). Therefore, we cannot exclude that the COOH-terminal part of CAN is localized in this position. However, the specificity of the anti-rat CAN antiserum for the *Xenopus* protein has not been reported. Biochemical identification of a nucleoporin subcomplex containing CAN/Nup214 and p62 (Finlay et al., 1991; Matsuoka et al., 1999) is consistent with the localization of CAN/Nup214 at the cytoplasmic face of the translocation channel. p62 itself has been localized at both entrances of the NPC translocation channel using preembedding (Cordes et al., 1995; Guan et al., 1995) and postembedding immuno-TEM (Grote et al., 1995). Our study shows a CAN/Nup214 localization similar to the localization of Nup159/Rat7 (Kraemer et al., 1995; Rout et al., 2000), the closest yeast homologue to vertebrate CAN/Nup214, suggesting a greater degree of functional conservation between these two nucleoporins than could earlier be assumed. The position of CAN/Nup214 close to the translocation channel may allow its FG repeats to contribute to the hydrophobic FG repeat network that is hypothesized to fill the translocation channel (Grote et al., 1995; Ribbeck and Gorlich, 2001).

Decoration with two different antibodies localized RanBP2/Nup358 on the cytoplasmic filaments of the NPC, in agreement with previous studies (Wilken et al., 1995; Wu et al., 1995; Yokoyama et al., 1995). Two additional lines of evidence suggest that RanBP2 is the major structural component of the cytoplasmic filaments. First, electron microscopic analysis of purified RanBP2 shows particles with a filamentous shape and a length of ~36 nm, which is both consistent with the approximate size of the cytoplasmic filaments and the length of RanBP2's amino acid sequence (Delphin et al., 1997). Second, depletion of RanBP2 leads to absence of filaments from the cytoplasmic face of the NPC.

The use of the two antibodies raised against different regions of RanBP2 in the same study has allowed us to com-

pare their localization relative to each other. The 358V antibodies recognize a small region corresponding to amino acids 2290–2314 of the human RanBP2 protein (Wu et al., 1995; Yokoyama et al., 1995), whereas the 358F antibodies recognize a region closer to the COOH terminus and correspond to amino acids 2501–2900. Our data show that the 358F epitopes are localized at a significantly more distal position than the 358V epitopes, suggesting that the protein is oriented with its COOH terminus pointing outward into the cytoplasm. Consequently, its NH<sub>2</sub> terminus, containing predicted coiled-coil and leucine zipper sequences (Wu et al., 1995; Yokoyama et al., 1995), may provide the interaction domains with the core NPC.

RanBP2/Nup358 is conserved among metazoa but absent in the yeast *Saccharomyces cerevisiae*. Therefore, it remains to be determined whether yeast contains cytoplasmic filaments that are functionally or structurally equivalent to those in metazoa.

### The cytoplasmic NPC filaments and nuclear import

Nuclei lacking CAN/Nup214 showed a relatively minor, 25% reduction in basic NLS-mediated protein import. Earlier studies in CAN  $-/-$  mouse embryos showed a 50% reduction in NLS protein import (van Deursen et al., 1996). Even though there is a difference in the degree of reduction between the two model systems, in both cases protein import is reduced but not eliminated. This is consistent with the situation in yeast, where mutations in Nup159/Rat7 have a limited effect on protein import (Del Priore et al., 1997; Belgareh et al., 1998; Hurwitz et al., 1998).

Most surprisingly, our results show that removal of RanBP2 and the complete cytoplasmic filaments affects neither NLS- or M9-mediated nuclear import, nor the exclusion of nonimport cargos. This holds true for multivalent exogenous cargos, as well as for the endogenous cargos Lamin LIII (Hennekes et al., 1993; Lourim and Krohne, 1993), Tpr (Cordes et al., 1998), and factors required for DNA replication (Walter et al., 1998). Also, Nup153, an endogenous cargo for transportin (Nakielny et al., 1999), was localized correctly. These results indicate that the cytoplasmic filaments do not act as essential docking sites for incoming import complexes as had been suggested previously (Newmeyer and Forbes, 1988; Richardson et al., 1988; Akey and Goldfarb, 1989; Moore and Blobel, 1992; Melchior et al., 1995; Pante and Aebi, 1996; Mahajan et al., 1997; Rutherford et al., 1997), and the efficient exclusion of BSA–SLN conjugate from depleted nuclei suggests they are also not required for entropic exclusion of nonkaryophilic proteins (Rout et al., 2000).

How can this conclusion be reconciled with previous data linking RanBP2 and the cytoplasmic filaments to an early step in protein import? EM studies have observed NLS cargo association with cytoplasmic NPC filaments during normal import (Newmeyer and Forbes, 1988; Richardson et al., 1988; Akey and Goldfarb, 1989), suggesting a temporal arrest. However, these studies have not addressed the necessity of these associations. A stronger indication that the cytoplasmic filaments were directly involved in import was the accumulation of NLS cargos at the NE, or more specifically at the filaments, under certain conditions including depletion of NTPs or Ran, addition of O-linked N-acetylglucosamine

binding lectin, or chilling to 4°C (Dabauvalle et al., 1988; Featherstone et al., 1988; Richardson et al., 1988; Moore and Blobel, 1992; Chi et al., 1996; Rutherford et al., 1997). As argued previously (Englmeier et al., 1999), the perinuclear accumulation of classical NLS substrates observed under conditions that deplete NTPs or Ran (Newmeyer et al., 1986; Richardson et al., 1988; Moore and Blobel, 1992; Melchior et al., 1995) is likely the result of depletion of RanGTP that is needed to dissociate importin $\alpha$ - $\beta$ /cargo complexes from the NPC (Rexach and Blobel, 1995; Gorlich et al., 1996). This accumulation may block the translocation channel (Kutay et al., 1997). Chilling is likely to stabilize interactions of import complexes with NPC components, causing a similar block of the NPC with endogenous cargos (Englmeier et al., 1999). Lectin or antibody binding to carbohydrate moieties on some nucleoporins is also likely to arrest NPC translocation. Therefore, the observed “docking” of import complexes to the cytoplasmic filaments under these conditions may be caused by obstruction of nucleoporin sites within the NPC that mediate the import reaction. By blocking these, import complexes may associate or reassociate with sites that would normally not contribute to the import reaction, but serve another function. In this regard it is noteworthy that the FG repeats in RanBP2 are relatively sparse (Wu et al., 1995; Yokoyama et al., 1995), and have a low affinity for importin  $\beta$  (Ben-Efraim and Gerace, 2001). Alternatively, the association of import complexes with the filaments may function to concentrate them in the vicinity of the core NPC, increasing import efficiency (Rout et al., 2000; Ben-Efraim and Gerace, 2001). However, we have not detected reduced import rates due to lack of RanBP2 or cytoplasmic filaments, whereas we did detect a reduction in NLS-mediated import due to depletion of CAN/Nup214.

The association of Ran with the cytoplasmic filaments in the presence of nonhydrolysable GTP analogs (Melchior et al., 1995), can be explained by binding of RanGTP to the RBD domains of RanBP2 and does not necessarily represent an early step of nuclear import. Transport induced bending of the cytoplasmic filaments, described as a mechanism for import (Pante and Aebi, 1996; Rutherford et al., 1997) may be caused by the multivalence of the transport substrates that were employed in these studies. NLS-coated gold particles are likely to interact with multiple copies of importin  $\beta$ , enabling them to occasionally link FG repeats at the entrance of the translocation channel (e.g., those of CAN/Nup214 or p62), to those of RanBP2.

Polyclonal antibodies raised against a GST-fused RanBP2 fragment comprising two of the RanGTP binding domains plus several Zinc fingers and FG repeats inhibited nuclear import of an NLS containing substrate (Yokoyama et al., 1995). Even though we cannot exclude that certain antibodies to RanBP2/Nup358 interfere specifically with NLS import, these antibodies also labeled the nuclear face of the NPC (Yokoyama et al., 1995), suggesting that they may have crossreacted with other Zinc finger or FG repeat containing nucleoporins such as Nup153 or p62.

In conclusion, our data argue against an essential role of the cytoplasmic NPC filaments in NLS and M9 dependent protein import, and by default support translocation models that do not involve them (Rexach and Blobel, 1995; Ben-Efraim

and Gerace, 2001; Ribbeck and Gorlich, 2001). It remains possible that the cytoplasmic filaments are required for import of cargos not imported via the classical NLS- and M9-import pathways, or for very large cargos, although the experiments in which we coated RanBP2 with colloidal gold-labeled antibodies without affecting the import of substrates of diameter between 10–16 nm would argue against the latter.

It is noteworthy that the cyclophilin-like domain of RanBP2 has been shown to interact with the 19S regulatory particle of the 26S proteasome (Ferreira et al., 1998). The 19S particle is known to have unfolding/chaperone activity. Specific binding to RanBP2 may indicate a demand for an unfolding activity at the cytoplasmic periphery of the NPC. Although such an activity seems unlikely to be required for NPC translocation it may serve some other function. A further property of RanBP2 which may not be directly related to the actual nuclear translocation process is the recently identified ability of RanBP2 to act as a SUMO-1 E3 ligase (Pichler et al., 2002). With the exception of RanGAP1 (Matunis et al., 1996; Mahajan et al., 1997; Matunis et al., 1998) and RanBP2 itself (Pichler et al., 2002), all known sumoylated proteins are predominately nuclear (for review see Muller et al., 2001). The association of import cargos with the filaments therefore may represent a temporal transport arrest to allow modification of specific cargos, rather than a general facilitating step in nuclear import.

## Materials and methods

### Antibodies

Anti-RanBP2 antibodies (358V) were raised in guinea pig against a peptide corresponding to amino acids 2285–2314 of human RanBP2 (Wu et al., 1995; Yokoyama et al., 1995) of which aa 2290–2314 are identical to a partial sequence of RanBP2 from *Xenopus laevis* (GenBank/EMBL/DBJ accession no. BG233383). The peptide was coupled via an NH<sub>2</sub>-terminal cysteine residue to maleimide-activated keyhole limpet hemocyanin and used for immunization as described (Cordes et al., 1997b). For affinity purification of Igs, the peptide was coupled to Ultra Link Iodoacetyl on 3M Emphaze Biosupport Medium AB1 (Pierce Chemical Co.) and purified as described (Cordes et al., 1997b). Antiserum 358F was provided by A. Gast and F. Melchior (Max Planck Institute for Biochemistry, Munich, Germany). To generate specific antibodies against *Xenopus* CAN (anti-214) an NH<sub>2</sub>-terminal fragment spanning amino acids 1–213 of the published sequence (Askjaer et al., 1999) was expressed as a His6-tagged fusion protein in pQE31 (QIAGEN) in XL1-Blue and purified under denaturing conditions. Antibodies were raised in rabbits and affinity purified against the antigen crosslinked to Affigel-15 (Biorad). To generate a resin for the depletion from *Xenopus* egg extracts, saturating amounts of antibody were bound to protein A Sepharose (Amersham Pharmacia Biotech) and crosslinked with 10 mM dimethylpimelidate (Sigma-Aldrich).

### Preparation of colloidal gold-coupled proteins

Coupling to 5-nm colloidal gold, as well as preparation of BSA-SV40NLS conjugates and their coupling to 10-nm colloidal gold was performed essentially as described (Cordes et al., 1997a). To avoid overloads of protein which may result in subsequent leaching of bound material, Igs or BSA-SV40NLS were added to the gold particles at amounts just sufficient to maintain colloidal stability upon addition of NaCl (Slot and Geuze, 1984). Remaining binding sites were blocked by incubating the gold suspension with 0.1% BSA for 15 min before dilution in 20 vol of injection buffer (88 mM NaCl, 1 mM KCl, 20 mM Hepes, pH 7.4). To remove the excess of unbound protein, the suspension was centrifuged at 10,000 g for 1 or 2 h, depending on particle size. The supernatant and an occasionally observed minor solid pellet consisting of coagulated gold were discarded, whereas the fluffy and very loose major part of the sediment, containing the gold conjugates in colloidal form, was resuspended in injection buffer and washed again. Following final centrifugation, the loose sediment was collected as a concentrated, black suspension and used either directly for injection or stored at 4°C.

### Microinjection and electron microscopy of injected oocytes

Microinjections into the cytoplasm of nondefolliculated *Xenopus* stage VI oocytes were performed at room temperature essentially as described (Cordes et al., 1997a). Four to six oocytes were injected for each experiment. Injections of gold-coupled antibodies were done at two sites opposite to each other at the equatorial borderline between animal and vegetal hemisphere. Injections of gold-coupled BSA-SV40NLS, or of gold-coupled BSA without NLS as control, were performed at a single site near the pole of the vegetal hemisphere. Oocytes were then incubated in modified Barth's medium at either 2°C in the cold room or in a 19°C incubator for 3, 5, 8, 16, 22, or 30 h. For experiments in which antibody injections preceded the injection of gold-coupled BSA-SV40NLS, oocytes injected with 5-nm gold anti-RanBP2, or mock-injected with buffer alone, were first incubated at 2°C for 16 h. Following subsequent injection of 10-nm gold BSA-SV40NLS, oocytes were further incubated at 19°C for 6 h. Oocytes were then fixed in glutaraldehyde and processed for electron microscopy exactly as described (Cordes et al., 1997a).

### EM immunolocalization

Immunolocalization of Nup214 and Nup358 on isolated *Xenopus* oocyte NEs using TEM and FEISEM was performed as previously described (Walther et al., 2001). For FEISEM analysis, antibodies were diluted 1:100 with PBS before being incubated with isolated *Xenopus* oocyte NEs. The 214 and 358F primary antibodies were labeled with 10-nm gold-conjugated anti-rabbit secondary antibodies and the 358V antibody with 10-nm gold-conjugated anti-guinea pig antibody (Amersham Pharmacia Biotech), all at 1:20 dilution. Negative controls were performed and revealed the secondary antibodies to be specific (unpublished data). Isolated NEs were visualized at 100–300 kx magnification. To quantify the immunolocalization, measurements were made using AnalySIS (SIS) software. For TEM quantification, the midplane of the NE (i.e., a line parallel to the NE and equidistant from both the inner and outer nuclear membranes) for each NPC was determined. The distances between the midplane of the NE and the gold-labeled antibodies were measured at right angles to the midplane. For quantification of the position of nucleoporins by FEISEM, the gold-labeled antibodies were identified on the secondary electron image from the corresponding backscatter image. Circles of best fit were placed over each NPC and each gold-labeled antibody, and the distances between the center of the NPCs and the center of the gold-labeled antibodies were measured.

### FEISEM analysis of depleted nuclei

After nuclear assembly, 4  $\mu$ l of the assembly reaction was diluted with 1 ml MWB250 (250 mM sucrose, 50 mM KCl, 2.5 mM MgCl<sub>2</sub>, 50 mM Hepes, pH 8), and nuclei were spun down onto silicon chips at 800 g and fixed in membrane fix (80 mM Pipes, pH 6.8; 1 mM MgCl<sub>2</sub>; 150 mM sucrose; 2% paraformaldehyde; 0.5% glutaraldehyde), for 30 min at room temperature. Samples were postfixed with 1% (wt/vol) OsO<sub>4</sub>, 0.2 M cacodylate, pH 7.4, and 1% (wt/vol) aqueous uranyl acetate for 10 min each, dehydrated through an ethanol series, and critical point dried from high purity CO<sub>2</sub>. Samples were sputter coated with 3 nm chromium and viewed using a Topcon DS130F FEISEM (Topcon Corporation) at 30 kV accelerating voltage.

### Nuclear assembly, import and replication assays, and indirect immunofluorescence

Fractionated egg extracts were prepared and depleted as described (Walther et al., 2001) except that the cytosolic fraction was depleted by two incubations with an equal volume of mock, anti-214, anti-RanBP2(358V), or a mixture of anti-214 and anti-RanBP2 resin, which was preblocked with 5% BSA for 1 h. Assembly, import, and immunofluorescence reactions were performed as described (Hetzer et al., 2000). In brief, for a 200- $\mu$ l reaction, 13.5  $\mu$ l cytosol, 1.5  $\mu$ l energy mix (10 mM ATP, 100 mM creatine phosphate, 2 mg/ml creatine kinase), 20 mg/ml glycogen (USB; Amersham Pharmacia Biotech) were mixed. 1  $\mu$ l sperm chromatin followed by 2  $\mu$ l of membrane fraction were added and the reaction incubated for 2 h at 20°C. For nuclear import reactions, a fluorescently labeled BSA-NLS conjugate (Palacios et al., 1996) or Nplc-M9-M10 (Englmeier et al., 1999) and an inert control substrate (BSA-SLN) were added and further incubated for various times. The samples were subsequently fixed in 4% formaldehyde and centrifuged through a cushion of 30% (wt/vol) sucrose onto an L-polylysine-coated coverslip and either directly monitored by confocal microscopy or further processed for immunofluorescence as described (Arts et al., 1997). *Xenopus* RanGAP1 was detected by an antiserum provided by M. Dasso (National Institutes of Health, Bethesda, MD), Nup98 with an antiserum to human Nup98 (Wu et al., 2001) that recog-

nizes *Xenopus* Nup98 (unpublished data), Tpr with purified antipeptide antibodies (Cordes et al., 1997b), Lamin III with monoclonal antibody S49 (Lourin and Krohne, 1993), and Nup153 as described (Walther et al., 2001). Images were recorded with a Zeiss LSM 510 or a Leica TCS confocal microscope. Import reactions were quantified using NIH Image. The mean fluorescence of 10 or more images containing several nuclei each was determined. Error bars represent standard errors. DAPI staining for chromatin was used to verify that quantified objects were nuclei. Replication of DNA was assayed by addition of 40  $\mu$ M 21-Biotin-dUTP (CLONTECH Laboratories, Inc.) to the nuclear assembly reactions in the presence or absence of 14  $\mu$ M of aphidicolin (Sigma-Aldrich). Samples were treated as for immunofluorescence microscopy and incorporated biotin was detected with Alexa 488-linked streptavidin (Molecular Probes).

We gratefully acknowledge Dr. Hans-Richard Rackwitz for advice and help in colloidal gold-labeling of proteins, Drs. Andreas Gast and Frauke Melchior (Max Planck Institute for Biochemistry, Munich, Germany) for producing and characterizing the anti-RanBP2 358F antibodies, and Drs. Mary Dasso and Jan van Deursen for antisera to RanGAP1 and Nup98. We thank Martin Hetzer and Wolfram Antonin for discussions and Elisa Izauralde, and Jan Ellenberg and members of the Mattaj laboratory for suggestions on the manuscript. Many thanks also to Sonja Reidenbach and Sandra Rutherford for technical assistance.

H.S. Pickersgill, M.W. Goldberg, and T.D. Allen were supported by Cancer Research UK.

Submitted: 19 February 2002

Revised: 29 April 2002

Accepted: 24 May 2002

## References

- Akey, C.W. 1989. Interactions and structure of the nuclear pore complex revealed by cryo-electron microscopy. *J. Cell Biol.* 109:955–970.
- Akey, C.W., and D.S. Goldfarb. 1989. Protein import through the nuclear pore complex is a multistep process. *J. Cell Biol.* 109:971–982.
- Akey, C.W., and M. Radermacher. 1993. Architecture of the *Xenopus* nuclear pore complex revealed by three-dimensional cryo-electron microscopy. *J. Cell Biol.* 122:1–19.
- Allen, T.D., J.M. Cronshaw, S. Bagley, E. Kiseleva, and M.W. Goldberg. 2000. The nuclear pore complex: mediator of translocation between nucleus and cytoplasm. *J. Cell Sci.* 113:1651–1659.
- Arts, G.J., L. Englmeier, and I.W. Mattaj. 1997. Energy- and temperature-dependent *in vitro* export of RNA from synthetic nuclei. *Biol. Chem.* 378:641–649.
- Askjaer, P., A. Bachi, M. Wilm, F.R. Bischoff, D.L. Weeks, V. Ogniewski, M. Ohno, C. Niehrs, J. Kjems, I.W. Mattaj, and M. Fornerod. 1999. RanGTP-regulated interactions of CRM1 with nucleoporins and a shuttling DEAD-box helicase. *Mol. Cell Biol.* 19:6276–6285.
- Bastos, R., L. Ribas de Pouplana, M. Enarson, K. Bodoor, and B. Burke. 1997. Nup84, a novel nucleoporin that is associated with CAN/Nup214 on the cytoplasmic face of the nuclear pore complex. *J. Cell Biol.* 137:989–1000.
- Beddow, A.L., S.A. Richards, N.R. Orem, and I.G. Macara. 1995. The Ran/TC4 GTPase-binding domain: identification by expression cloning and characterization of a conserved sequence motif. *Proc. Natl. Acad. Sci. USA.* 92:3328–3332.
- Belgareh, N., C. Snay-Hodge, F. Pasteau, S. Dagher, C.N. Cole, and V. Doye. 1998. Functional characterization of a Nup159p-containing nuclear pore subcomplex. *Mol. Biol. Cell.* 9:3475–3492.
- Ben-Efraim, I., and L. Gerace. 2001. Gradient of increasing affinity of importin beta for nucleoporins along the pathway of nuclear import. *J. Cell Biol.* 152:411–417.
- Bischoff, F.R., and D. Gorlich. 1997. RanBP1 is crucial for the release of RanGTP from importin beta-related nuclear transport factors. *FEBS Lett.* 419:249–254.
- Bischoff, F.R., H. Krebber, E. Smirnova, W. Dong, and H. Ponstingl. 1995. Co-activation of RanGTPase and inhibition of GTP dissociation by Ran-GTP binding protein RanBP1. *EMBO J.* 14:705–715.
- Blow, J.J., and R.A. Laskey. 1986. Initiation of DNA replication in nuclei and purified DNA by a cell-free extract of *Xenopus* eggs. *Cell.* 47:577–587.
- Chi, N.C., E.J. Adam, G.D. Visser, and S.A. Adam. 1996. RanBP1 stabilizes the interaction of Ran with p97 nuclear protein import. *J. Cell Biol.* 135:559–569.
- Cordes, V.C., S. Reidenbach, and W.W. Franke. 1995. High content of a nuclear pore complex protein in cytoplasmic annulate lamellae of *Xenopus* oocytes. *Eur. J. Cell Biol.* 68:240–255.
- Cordes, V.C., H.R. Rackwitz, and S. Reidenbach. 1997a. Mediators of nuclear protein import target karyophilic proteins to pore complexes of cytoplasmic annulate lamellae. *Exp. Cell Res.* 237:419–433.
- Cordes, V.C., S. Reidenbach, H.R. Rackwitz, and W.W. Franke. 1997b. Identification of protein p270/Tpr as a constitutive component of the nuclear pore complex-attached intranuclear filaments. *J. Cell Biol.* 136:515–529.
- Cordes, V.C., M.E. Hase, and L. Muller. 1998. Molecular segments of protein Tpr that confer nuclear targeting and association with the nuclear pore complex. *Exp. Cell Res.* 245:43–56.
- Dabauvalle, M.C., B. Schulz, U. Scheer, and R. Peters. 1988. Inhibition of nuclear accumulation of karyophilic proteins in living cells by microinjection of the lectin wheat germ agglutinin. *Exp. Cell Res.* 174:291–296.
- Delphin, C., T. Guan, F. Melchior, and L. Gerace. 1997. RanGTP targets p97 to RanBP2, a filamentous protein localized at the cytoplasmic periphery of the nuclear pore complex. *Mol. Biol. Cell.* 8:2379–2390.
- Del Priore, V., C. Heath, C. Snay, A. MacMillan, L. Gorsch, S. Dagher, and C. Cole. 1997. A structure/function analysis of Rat7p/Nup159p, an essential nucleoporin of *Saccharomyces cerevisiae*. *J. Cell Sci.* 110:2987–2999.
- Englmeier, L., J.C. Olivo, and I.W. Mattaj. 1999. Receptor-mediated substrate translocation through the nuclear pore complex without nucleotide triphosphate hydrolysis. *Curr. Biol.* 9:30–41.
- Fahrenkrog, B., D. Stoffler, and U. Aebi. 2001. Nuclear pore complex architecture and functional dynamics. *Curr. Top. Microbiol. Immunol.* 259:95–117.
- Featherstone, C., M.K. Darby, and L. Gerace. 1988. A monoclonal antibody against the nuclear pore complex inhibits nucleocytoplasmic transport of protein and RNA *in vivo*. *J. Cell Biol.* 107:1289–1297.
- Feldherr, C.M., E. Kallenbach, and N. Schultz. 1984. Movement of a karyophilic protein through the nuclear pores of oocytes. *J. Cell Biol.* 99:2216–2222.
- Ferreira, P.A., C. Yunfei, D. Schick, and R. Roepman. 1998. The cyclophilin-like domain mediates the association of Ran-binding protein 2 with subunits of the 19 S regulatory complex of the proteasome. *J. Biol. Chem.* 273:24676–24682.
- Finlay, D.R., and D.J. Forbes. 1990. Reconstitution of biochemically altered nuclear pores: transport can be eliminated and restored. *Cell.* 60:17–29.
- Finlay, D.R., E. Meier, P. Bradley, J. Horecka, and D.J. Forbes. 1991. A complex of nuclear pore proteins required for pore function. *J. Cell Biol.* 114:169–183.
- Floer, M., G. Blobel, and M. Rexach. 1997. Disassembly of RanGTP-karyopherin beta complex, an intermediate in nuclear protein import. *J. Biol. Chem.* 272:19538–19546.
- Fornerod, M., J. van Deursen, S. van Baal, A. Reynolds, D. Davis, K.G. Murti, J. Franssen, and G. Grosveld. 1997. The human homologue of yeast CRM1 is in a dynamic subcomplex with CAN/Nup214 and a novel nuclear pore component Nup88. *EMBO J.* 16:807–816.
- Goldberg, M.W., and T.D. Allen. 1993. The nuclear pore complex: three-dimensional surface structure revealed by field emission, in-lens scanning electron microscopy, with underlying structure uncovered by proteolysis. *J. Cell Sci.* 106:261–274.
- Goldberg, M.W., and T.D. Allen. 1996. The nuclear pore complex and lamina: three-dimensional structures and interactions determined by field emission in-lens scanning electron microscopy. *J. Mol. Biol.* 257:848–865.
- Goldberg, M.W., C. Wiese, T.D. Allen, and K.L. Wilson. 1997. Dimples, pores, star-rings, and thin rings on growing nuclear envelopes: evidence for structural intermediates in nuclear pore complex assembly. *J. Cell Sci.* 110:409–420.
- Gorlich, D., N. Pante, U. Kutay, U. Aebi, and F.R. Bischoff. 1996. Identification of different roles for RanGDP and RanGTP in nuclear protein import. *EMBO J.* 15:5584–5594.
- Grandi, P., T. Dang, N. Pane, A. Shevchenko, M. Mann, D. Forbes, and E. Hurt. 1997. Nup93, a vertebrate homologue of yeast Nic96p, forms a complex with a novel 205-kDa protein and is required for correct nuclear pore assembly. *Mol. Biol. Cell.* 8:2017–2038.
- Grote, M., U. Kubitscheck, R. Reichelt, and R. Peters. 1995. Mapping of nucleoporins to the center of the nuclear pore complex by post-embedding immunogold electron microscopy. *J. Cell Sci.* 108:2963–2972.
- Guan, T., S. Muller, G. Klier, N. Pante, J.M. Blevitt, M. Haner, B. Paschal, U. Aebi, and L. Gerace. 1995. Structural analysis of the p62 complex, an assembly of O-linked glycoproteins that localizes near the central gated channel of the nuclear pore complex. *Mol. Biol. Cell.* 6:1591–1603.
- Hennekes, H., M. Peter, K. Weber, and E.A. Nigg. 1993. Phosphorylation on protein kinase C sites inhibits nuclear import of Lamin B2. *J. Cell Biol.* 123:1293–1304.
- Hetzer, M., D. Bilbao-Cortes, T.C. Walther, O.J. Gruss, and I.W. Mattaj. 2000. GTP hydrolysis by Ran is required for nuclear envelope assembly. *Mol. Cell.* 5:1013–1024.
- Hinshaw, J.E., B.O. Carragher, and R.A. Milligan. 1992. Architecture and design

- of the nuclear pore complex. *Cell*. 69:1133–1141.
- Hurwitz, M.E., C. Strambio-de-Castilla, and G. Blobel. 1998. Two yeast nuclear pore complex proteins involved in mRNA export form a cytoplasmically oriented subcomplex. *Proc. Natl. Acad. Sci. USA*. 95:11241–11245.
- Jarnik, M., and U. Aebi. 1991. Toward a more complete 3-D structure of the nuclear pore complex. *J. Struct. Biol.* 107:291–308.
- Kehlenbach, R.H., A. Dickmanns, A. Kehlenbach, T. Guan, and L. Gerace. 1999. A role for RanBP1 in the release of CRM1 from the nuclear pore complex in a terminal step of nuclear export. *J. Cell Biol.* 145:645–657.
- Kraemer, D., R.W. Wozniak, G. Blobel, and A. Radu. 1994. The human CAN protein, a putative oncogene product associated with myeloid leukemogenesis, is a nuclear pore complex protein that faces the cytoplasm. *Proc. Natl. Acad. Sci. USA*. 91:1519–1523.
- Kraemer, D.M., C. Strambio-de-Castilla, G. Blobel, and M.P. Rout. 1995. The essential yeast nucleoporin NUP159 is located on the cytoplasmic side of the nuclear pore complex and serves in karyopherin-mediated binding of transport substrate. *J. Biol. Chem.* 270:19017–19021.
- Kutay, U., E. Izaurralde, F.R. Bischoff, I.W. Mattaj, and D. Gorlich. 1997. Dominant-negative mutants of importin-beta block multiple pathways of import and export through the nuclear pore complex. *EMBO J.* 16:1153–1163.
- Kutay, U., G. Lipowsky, E. Izaurralde, F.R. Bischoff, P. Schwarzmaier, E. Hartmann, and D. Gorlich. 1998. Identification of a tRNA-specific nuclear export receptor. *Mol. Cell*. 1:359–369.
- Lourim, D., and G. Krohne. 1993. Membrane-associated lamins in *Xenopus* egg extracts: identification of two vesicle populations. *J. Cell Biol.* 123:501–512.
- Mahajan, R., C. Delphin, T. Guan, L. Gerace, and F. Melchior. 1997. A small ubiquitin-related polypeptide involved in targeting RanGAP1 to nuclear pore complex protein RanBP2. *Cell*. 88:97–107.
- Matsuoka, Y., M. Takagi, T. Ban, M. Miyazaki, T. Yamamoto, Y. Kondo, and Y. Yoneda. 1999. Identification and characterization of nuclear pore subcomplexes in mitotic extract of human somatic cells. *Biochem. Biophys. Res. Commun.* 254:417–423.
- Matunis, M.J., E. Coutavas, and G. Blobel. 1996. A novel ubiquitin-like modification modulates the partitioning of the Ran-GTPase-activating protein RanGAP1 between the cytosol and the nuclear pore complex. *J. Cell Biol.* 135:1457–1470.
- Matunis, M.J., J. Wu, and G. Blobel. 1998. SUMO-1 modification and its role in targeting the Ran GTPase-activating protein, RanGAP1, to the nuclear pore complex. *J. Cell Biol.* 140:499–509.
- Meier, J., K. Campbell, C. Ford, R. Stick, and C. Hutchison. 1991. The role of Lamin LIII in nuclear assembly and DNA replication, in cell-free extracts of *Xenopus* eggs. *J. Cell Sci.* 98:271–279.
- Melchior, F., T. Guan, N. Yokoyama, T. Nishimoto, and L. Gerace. 1995. GTP hydrolysis by Ran occurs at the nuclear pore complex in an early step of protein import. *J. Cell Biol.* 131:571–581.
- Moore, M.S., and G. Blobel. 1992. The two steps of nuclear import, targeting to the nuclear envelope and translocation through the nuclear pore, require different cytosolic factors. *Cell*. 69:939–950.
- Muller, S., C. Hoegge, G. Pyrowolakis, and S. Jentsch. 2001. SUMO, ubiquitin's mysterious cousin. *Nat. Rev. Mol. Cell Biol.* 2:202–210.
- Nakielnny, S., S. Shaikh, B. Burke, and G. Dreyfuss. 1999. Nup153 is an M9-containing mobile nucleoporin with a novel Ran-binding domain. *EMBO J.* 18:1982–1995.
- Newmeyer, D.D., D.R. Finlay, and D.J. Forbes. 1986. In vitro transport of a fluorescent nuclear protein and exclusion of nonnuclear proteins. *J. Cell Biol.* 103:2091–2102.
- Newmeyer, D.D., and D.J. Forbes. 1988. Nuclear import can be separated into distinct steps in vitro: nuclear pore binding and translocation. *Cell*. 52:641–653.
- Ohno, M., M. Fornerod, and I.W. Mattaj. 1998. Nucleocytoplasmic transport: the last 200 nanometers. *Cell*. 92:327–336.
- Palacios, I., K. Weis, C. Klebe, I.W. Mattaj, and C. Dingwall. 1996. RAN/TC4 mutants identify a common requirement for snRNP and protein import into the nucleus. *J. Cell Biol.* 133:485–494.
- Pante, N., and U. Aebi. 1996. Sequential binding of import ligands to distinct nucleoporin regions during their nuclear import. *Science*. 273:1729–1732.
- Pante, N., R. Bastos, I. McMorro, B. Burke, and U. Aebi. 1994. Interactions and three-dimensional localization of a group of nuclear pore complex proteins. *J. Cell Biol.* 126:603–617.
- Pichler, A., A. Gast, J.S. Seeler, A. Dejean, and F. Melchior. 2002. The nucleoporin RanBP2 has SUMO1 E3 ligase activity. *Cell*. 108:109–120.
- Powers, M.A., C. Macaulay, F.R. Masiarz, and D.J. Forbes. 1995. Reconstituted nuclei depleted of a vertebrate GLFG nuclear pore protein, p97, import but are defective in nuclear growth and replication. *J. Cell Biol.* 128:721–736.
- Radu, A., M.S. Moore, and G. Blobel. 1995. The peptide repeat domain of nucleoporin Nup98 functions as a docking site in transport across the nuclear pore complex. *Cell*. 81:215–222.
- Rakowska, A., T. Danker, S.W. Schneider, and H. Oberleithner. 1998. ATP-induced shape change of nuclear pores visualized with the atomic force microscope. *J. Membr. Biol.* 163:129–136.
- Rexach, M., and G. Blobel. 1995. Protein import into nuclei: association and dissociation reactions involving transport substrate, transport factors, and nucleoporins. *Cell*. 83:683–692.
- Ribbeck, K., and D. Gorlich. 2001. Kinetic analysis of translocation through nuclear pore complexes. *EMBO J.* 20:1320–1330.
- Richards, S.A., K.M. Lounsbury, and I.G. Macara. 1995. The C terminus of the nuclear RAN/TC4 GTPase stabilizes the GDP-bound state and mediates interactions with RCC1, RAN-GAP, and HTF9A/RANBP1. *J. Biol. Chem.* 270:14405–14411.
- Richardson, W.D., A.D. Mills, S.M. Dilworth, R.A. Laskey, and C. Dingwall. 1988. Nuclear protein migration involves two steps: rapid binding at the nuclear envelope followed by slower translocation through nuclear pores. *Cell*. 52:655–664.
- Ris, H. 1989. Three-dimensional imaging of cell ultrastructure with high resolution low voltage SEM. *Inst. Physiol. Conf. Ser.* 98:657–662.
- Ris, H. 1991. The three-dimensional structure of the nuclear pore complex as seen by high voltage electron microscopy and high resolution low voltage scanning electron microscopy. *EMSA Bull.* 21:54–56.
- Ris, H. 1997. High-resolution field-emission scanning electron microscopy of nuclear pore complex. *Scanning*. 19:368–375.
- Ris, H., and M. Malecki. 1993. High-resolution field emission scanning electron microscope imaging of internal cell structures after Epon extraction from sections: a new approach to correlative ultrastructural and immunocytochemical studies. *J. Struct. Biol.* 111:148–157.
- Rout, M.P., and J.D. Aitchison. 2001. The nuclear pore complex as a transport machine. *J. Biol. Chem.* 276:16593–16596.
- Rout, M.P., J.D. Aitchison, A. Suprapto, K. Hjertaas, Y. Zhao, and B.T. Chait. 2000. The yeast nuclear pore complex: composition, architecture, and transport mechanism. *J. Cell Biol.* 148:635–651.
- Rutherford, S.A., M.W. Goldberg, and T.D. Allen. 1997. Three-dimensional visualization of the route of protein import: the role of nuclear pore complex substructures. *Exp. Cell Res.* 232:146–160.
- Ryan, K.J., and S.R. Wenthe. 2000. The nuclear pore complex: a protein machine bridging the nucleus and cytoplasm. *Curr. Opin. Cell Biol.* 12:361–371.
- Saitoh, H., C.A. Cooke, W.H. Burgess, W.C. Earnshaw, and M. Dasso. 1996. Direct and indirect association of the small GTPase ran with nuclear pore proteins and soluble transport factors: studies in *Xenopus laevis* egg extracts. *Mol. Biol. Cell*. 7:1319–1334.
- Schlenstedt, G., D.H. Wong, D.M. Koepf, and P.A. Silver. 1995. Mutants in a yeast Ran binding protein are defective in nuclear transport. *EMBO J.* 14:5367–5378.
- Schlenstedt, G., E. Smirnova, R. Deane, J. Solsbacher, U. Kutay, D. Gorlich, H. Ponstingl, and F.R. Bischoff. 1997. Yrb4p, a yeast ran-GTP-binding protein involved in import of ribosomal protein L25 into the nucleus. *EMBO J.* 16:6237–6249.
- Slot, J.W., and H.J. Geuze. 1984. Goldmarkers for single and double immunolabeling of ultrathin cryosections. In *Immunolabelling for Electron Microscopy*. J.M. Polak and I.M. Varndess, editors. Elsevier, New York.
- Spann, T.P., R.D. Moir, A.E. Goldman, R. Stick, and R.D. Goldman. 1997. Disruption of nuclear lamin organization alters the distribution of replication factors and inhibits DNA synthesis. *J. Cell Biol.* 136:1201–1212.
- Stoffler, D., B. Fahrenkrog, and U. Aebi. 1999a. The nuclear pore complex: from molecular architecture to functional dynamics. *Curr. Opin. Cell Biol.* 11:391–401.
- Stoffler, D., K.N. Goldie, B. Feja, and U. Aebi. 1999b. Calcium-mediated structural changes of native nuclear pore complexes monitored by time-lapse atomic force microscopy. *J. Mol. Biol.* 287:741–752.
- Sukegawa, J., and G. Blobel. 1993. A nuclear pore complex protein that contains zinc finger motifs, binds DNA, and faces the nucleoplasm. *Cell*. 72:29–38.
- Uv, A.E., P. Roth, N. Xylourgidis, A. Wickberg, R. Cantera, and C. Samakovlis. 2000. Members only encodes a *Drosophila* nucleoporin required for rel protein import and immune response activation. *Genes Dev.* 14:1945–1957.
- van Deursen, J., J. Boer, L. Kasper, and G. Grosveld. 1996. G2 arrest and impaired nucleocytoplasmic transport in mouse embryos lacking the proto-oncogene CAN/Nup214. *EMBO J.* 15:5574–5583.

- Vasu, S.K., and D.J. Forbes. 2001. Nuclear pores and nuclear assembly. *Curr. Opin. Cell Biol.* 13:363–375.
- Villa Braslavsky, C.I., C. Nowak, D. Gorlich, A. Wittinghofer, and J. Kuhlmann. 2000. Different structural and kinetic requirements for the interaction of Ran with the Ran-binding domains from RanBP2 and importin-beta. *Biochemistry.* 39:11629–11639.
- Walter, J., L. Sun, and J. Newport. 1998. Regulated chromosomal DNA replication in the absence of a nucleus. *Mol. Cell.* 1:519–529.
- Walther, T.C., M. Fornerod, H. Pickersgill, M.W. Goldberg, T.D. Allen, and I.W. Mattaj. 2001. The nucleoporin Nup153 is required for nuclear pore basket formation, nuclear pore complex anchoring and import of a subset of nuclear proteins. *EMBO J.* 20:5703–5714.
- Wilken, N., J.L. Senecal, U. Scheer, and M.C. Dabauvalle. 1995. Localization of the Ran-GTP binding protein RanBP2 at the cytoplasmic side of the nuclear pore complex. *Eur. J. Cell Biol.* 68:211–219.
- Wu, J., M.J. Matunis, D. Kraemer, G. Blobel, and E. Coutavas. 1995. Nup358, a cytoplasmically exposed nucleoporin with peptide repeats, Ran-GTP binding sites, zinc fingers, a cyclophilin A homologous domain, and a leucine-rich region. *J. Biol. Chem.* 270:14209–14213.
- Wu, X., L.H. Kasper, R.T. Mantcheva, G.T. Mantchev, M.J. Springett, and J.M. van Deursen. 2001. Disruption of the FG nucleoporin NUP98 causes selective changes in nuclear pore complex stoichiometry and function. *Proc. Natl. Acad. Sci. USA.* 98:3191–3196.
- Yang, L., T. Guan, and L. Gerace. 1997. Lamin-binding fragment of LAP2 inhibits increase in nuclear volume during the cell cycle and progression into S phase. *J. Cell Biol.* 139:1077–1087.
- Yaseen, N.R., and G. Blobel. 1999a. GTP hydrolysis links initiation and termination of nuclear import on the nucleoporin nup358. *J. Biol. Chem.* 274:26493–26502.
- Yaseen, N.R., and G. Blobel. 1999b. Two distinct classes of Ran-binding sites on the nucleoporin Nup-358. *Proc. Natl. Acad. Sci. USA.* 96:5516–5521.
- Yokoyama, N., N. Hayashi, T. Seki, N. Pante, T. Ohba, K. Nishii, K. Kuma, T. Hayashida, T. Miyata, U. Aebi, et al. 1995. A giant nucleopore protein that binds Ran/TC4. *Nature.* 376:184–188.